International Journal of Biological Macromolecules 113 (2018) 719–728

Contents lists available at ScienceDirect

International Journal of Biological Macromolecules

journal homepage: https://www.journals.elsevier.com/ijbiomac

Design of cellulose ether-based macromolecular prodrugs of ciprofloxacin for extended release and enhanced bioavailability

Muhammad Amin [a,1], Nazia Shahana Abbas [a,1], Muhammad Ajaz Hussain [a,*], Muhammad Sher [a], Kevin J. Edgar [b]

[a] Department of Chemistry, University of Sargodha, Sargodha 40100, Pakistan
[b] Department of Sustainable Biomaterials, Macromolecules and Interfaces Institute, Virginia Tech, 230 Cheatham Hall, Blacksburg, VA 24061, United States

ARTICLE INFO

Article history:
Received 6 January 2018
Received in revised form 13 February 2018
Accepted 22 February 2018
Available online 24 February 2018

Keywords:
Ciprofloxacin
Hydroxypropylcellulose
Hydroxyethylcellulose
Sustained release
Pharmacokinetics
Antibacterial activity
Cytotoxicity

ABSTRACT

The present study reveals the syntheses of hydroxypropylcellulose (HPC) and hydroxyethylcellulose (HEC) based macromolecular prodrugs (MPDs) of ciprofloxacin (CIP) using homogeneous reaction methodology. Covalently loaded drug content (DC) of each prodrug was quantified using UV–Vis spectrophotometry to determine degree of substitution (DS). HPC-ciprofloxacin (HPC-CIP) conjugates showed DS of CIP in the range 0.87–1.15 whereas HEC-ciprofloxacin (HEC-CIP) conjugates showed DS range 0.51–0.75. Transmission electron microscopy revealed that HPC-CIP conjugate **2** and HEC-CIP conjugate **6** self-assembled into nanoparticles of 150–300 and 180–250 nm, respectively. Size exclusion chromatography revealed HPC-CIP conjugate **2** and HEC-CIP conjugate **6** as monodisperse systems. In vitro drug release studies indicated 15 and 43% CIP release from HPC-CIP conjugate **2** after 6 h in simulated gastric and simulated intestinal fluids (SGF and SIF), respectively. HEC-CIP conjugate **6** showed 16% and 46% release after 6 h in SGF and SIF, respectively. HPC-CIP conjugate **2** and HEC-CIP conjugate **6** exhibited half-lives of 10.87 and 11.71 h, respectively with area under the curve values of 164 and 175 h μg mL^{-1}, respectively, indicating enhanced bioavailability and improved pharmacokinetic profiles in animal model. Equal antibacterial activities to that of unmodified CIP confirmed their competitive efficacies. Cytotoxicity studies supported their non-toxic nature and biocompatibility.

1. Introduction

Fluoroquinolone antibiotics [1] are very important therapeutics, and ciprofloxacin (CIP) in particular is the most widely prescribed antibiotic worldwide due to its broad spectrum of activity against various gram positive and gram negative bacteria [2–5]. Ciprofloxacin being zwitterionic exhibits pH dependent solubility and its hydrochloride (HCl) form shows its highest solubility at pH 4–5, with poor solubility in neutral water. Nevertheless, CIP solubility increases with increasing pH value [6]. Partition coefficient (log *P*) values of CIP have been reported as −0.94 and −1.70 in *n* octanol sodium phosphate buffer of pH 7.0 at 37 °C and pH 7.2 at 25 °C, respectively [7,8]. Ciprofloxacin is probably absorbed by passive diffusion in the upper GI tract, up to the jejunum [9]. CIP bioavailability is dose and route dependent. It was observed that CIP C_{max} value upon oral administration increased with increasing dose up to a certain level [10,11] because higher dose (750 mg kg^{-1}) showed identical bioavailability to that of 200 mg kg^{-1} dosage (69% vs. 69.1%) but with longer time to reach maximum concentration (t_{max}; 1.38 h vs. 0.69 h) indicating delayed absorption [12].

Therefore, it is of great importance to design CIP prodrugs to address the issues such as poor hydrophilicity, short half-life, poor systemic distribution, and low oral bioavailability of CIP [13–17].

Recently, macromolecular prodrugs (MPDs) of several therapeutic agents based on polysaccharides have been reported. These prodrugs offer a number of benefits, such as increased solubility of hydrophobic drug molecules [18], reduced dosage frequency [19,20], and improved pharmacokinetic profiles [21].

Among polysaccharides, cellulose ether derivatives have advantages as polymers from which to append drugs, to develop MPDs of different therapeutic agents for potential pharmaceutical applications [22–26]. The terminal hydroxyl groups of oligo(hydroxyalkyl) substituents on cellulose hydroxyalkyl ethers, i.e., hydroxypropylcellulose (HPC) and hydroxyethylcellulose (HEC), have wider approach angles than do the hydroxyls of the main cellulose chain, and can be esterified with carboxylic acid functional group-containing drugs [23,27]. These MPDs may act as substrates to esterase enzymes in vivo, and release active therapeutic agents after hydrolysis of ester linkages that are acid-, base-, and enzyme-labile [27–30]. Additionally, HPC and HEC are non-ionic, hydrophilic cellulose ether derivatives with low toxicity, biodegradable at certain DS and MS levels of substituent, and biocompatible in contact with the gastrointestinal (GI) tract. Therefore they find wide applications in the fields of pharmaceutics and drug delivery [23,31]. We hypothesize

* Corresponding author.
E-mail address: majaz172@yahoo.com (M.A. Hussain).
[1] Authors contributed equally.

https://doi.org/10.1016/j.ijbiomac.2018.02.142
0141-8130/

that HPC- and HEC-based prodrugs of CIP will have enhanced solubility vs. drug itself, will provide extended release enabled by hydrolysis of the ester linkage of drug to polymer, and will thereby afford enhanced CIP bioavailability.

The present work reports our efforts to synthesize HPC and HEC based MPDs of CIP. We also report a drug release study to establish these novel MPDs of CIP as sustained release vehicles. In addition, we describe pharmacokinetic studies of both conjugates in rabbit models. Antimicrobial activity and cytotoxicity of these novel conjugates were also investigated to establish their therapeutic efficacy and safety.

2. Materials and methods

2.1. Materials

US Pharmacopoeia standard CIP was acquired from Beijing Mesochem Technology Co, Ltd. Beijing, China. HPC (DS(HP) 3.00, MS (HP) 3.46) was obtained from Nanjing Yeshun Industry and International Trading Co. Ltd., Jiangsu, China. HEC (Natrosol™ HEC: DS(HE) 1.5, MS(HE) 2.5) was obtained from Ashland Inc., Covington, KY, USA. Polymers were dried under vacuum at 50 °C for 5 h before use. 4-Methylbenzenesulfonyl chloride (TsCl), triethylamine (TEA), *N,N′*-dimethylacetamide (DMAc), simulated gastric fluid (SGF, pH 1.2), and simulated intestinal fluid (SIF, pH 7.4) were purchased from Sigma-Aldrich. Diethyl ether and ethanol were obtained from Riedel-de Haën. All organic solvents and reagents used during syntheses were of analytical grade and used without further purification. TEM grids (Cu-200 CK) were acquired from Pacific Grid Tech, San Francisco, CA, USA. Cellu•Sep® dialysis membranes were obtained from Membrane Filtration Products, Inc. Seguin, TX, USA. Disposable Injekt™ syringes were of B. Braun Medical Inc. USA. VACUETTE® blood collection tubes were of Greiner Bio-One North America, Inc. Sartorius™ polyamide (nylon) membrane filters (0.45 μm × 115 μm × 90 mm) and Target2™ nylon syringe filters (0.45 μm × 30 mm) for HPLC were obtained from Fisher Scientific, Pittsburgh, PA, USA.

2.2. Measurements

FT-IR spectroscopy was carried out using an IR-Prestige 21 instrument (Shimadzu, Japan). The sample pellets were dried at 50 °C under vacuum before analysis. ^{1}H NMR spectra (16–64 scans) were acquired on a Bruker Avance II instrument operating at 500 MHz in deuterated solvents using TMS as an internal standard. ^{13}C NMR spectra (5000 scans at 50 °C) were acquired on an Agilent U4-DD2 instrument (400 MHz). MestReNova-8.0.2 software was used to process the spectral data. A PharmaSpec UV-1700 spectrophotometer (Shimadzu, Japan) was employed to estimate drug content (DC) of each conjugate. Standard and sample solutions were prepared in 0.1 N aq. NaOH and absorbance was recorded at λ_{max} (272 nm) of CIP. Nano-assembly behaviour of MPDs of CIP was studied at the DMSO/H_2O interface using a Philips 420 transmission electron microscope with accelerated voltage of 120 kV. Agilent Technologies 1200 (Germany) series size exclusion chromatography (SEC) equipment was used for molecular weight determination. The SEC instrument was equipped with a refractive index detector (G-1362A), G1311A quaternary pump, G1322A Degasser, G1315B DAD variable wavelength UV detector and 1200 system controller (all from Agilent, Germany).

In vitro release profile of CIP from conjugates was studied on a PT-DT USP Dissolution II Apparatus (PharmaTest, Germany) using simulated gastric and intestinal fluids (SGF; pH 1.2 and SIF; pH 7.4) to mimic in vivo drug release profile. Pharmacokinetic profiles of CIP MPDs were investigated by a simple, rapid, reverse phase HPLC/UV method that was also validated as per ICH guidelines. The HPLC instrument (Agilent Technologies 1200 Series, Germany) was equipped with G1322A degasser, G1311A Pump, and G1315B DAD variable wavelength UV detector.

2.3. Syntheses of HPC- and HEC-CIP conjugates

2.3.1. Typical procedure for the synthesis of HPC-CIP conjugate (Sample 2)

Pre-dried HPC (1.0 g, 2.75 mmol) was dissolved in DMAc (30 mL) by stirring for 30 min at 80 °C. TEA (2.30 mL, 16.52 mmol) and TsCl (1.58 g, 8.26 mmol) were added to the HPC solution followed by the addition of CIP (2.74 g, 8.26 mmol). The solution was stirred for 24 h under nitrogen at 80 °C. The cooled reaction mixture was added to diethyl ether (200 mL) for precipitation and isolation (filtration) of the product. The precipitates were washed with ethanol (100 mL) thrice and dried under vacuum for 24 h at 50 °C.

Yield = 1.76 g, 88%; DS(CIP) = 1.15.

FT-IR = 1731 cm^{-1} (CO_{Ester}), 2812–3051 cm^{-1} (CH and free OH), 1468 cm^{-1} (CH_2).

^{1}H NMR (δ ppm, 500 MHz, DMSO d_6) = 0.992 (H-9), 8.62 (*H*−10), 7.87 (*H*−11), 7.54 (*H*−12), 3.37 (*H*−13), 3.06 (H-14), 3.76 (H-15), 1.10 (H-16), 1.28 (H-17), 2.06 (H-18), 2.85–4.74 (HPC repeating unit-H-1-8).

^{13}C NMR (δ ppm, 400 MHz, DMSO d_6, NS 5000) = 102.69 (C-1), 74.91 (C-2 and C-7), 65.45 (C-6 and C-8), 76.53–82.78 (C-3-5), 21.49 (C-9), 111.56 (C-10), 154.62 (C-11), 139.46 (C-12), 107.55 (C-13,17), 148.56 (C-14), 119.63(C-15), 176.80 (C-16), 144.39 (C-18), 163.74 (C-19), 36.32 (C-20), 8.00 (C-21,22), 49.190 (C-23,26), 8.57 (C-23), 46.03 (C-24,25).

Spectroscopic data of HPC-CIP conjugates **1**, **3** and **4** is shown in supplementary information.

2.3.5. Typical procedure for synthesis of HEC-CIP conjugates (Sample 6)

CIP (3.60 g, 10.86 mmol) was added in parts to an HEC (1.0 g, 3.62 mmol) solution in DMAc (30 mL) containing TEA (3.03 mL, 21.72 mmol) and tosyl chloride (2.07 g, 10.86 mmol). The reaction mixture was stirred for 24 h at 80 °C under a nitrogen atmosphere. The cooled reaction mixture was added to diethyl ether (200 mL) to precipitate the product, which was isolated by filtration, washed thrice with ethanol (100 mL), and dried under vacuum for 24 h at 50 °C.

Yield = 1.60 g, 86%; DS(CIP) = 0.75.

FT-IR = 1737 cm^{-1} (CO_{Ester}), 2870–3082 cm^{-1} (aromatic and non-aromatic CH Stretch), 1458 cm^{-1} (CH_2 bend), 3189–3600 cm^{-1} (OH stretch of H-bonded groups).

^{1}H NMR (δ ppm, 500 MHz, DMSO d_6) = 8.66 (H-10), 7.86 (H-11), 7.51 (H-12), 3.65 (H-13), 3.36 (H-14), 3.78 (H-15), 1.19 (H-16), 1.32 (H-17), 2.01 (H-18), 3.05–4.78 (HEC repeating unit-H-1-9).

^{13}C NMR (δ ppm, 400 MHz, DMSO d_6, NS 5000) = 102.15–103.04 (C-1), 78.14–82.83 (C-2-4), 74.72.-72.77 (C-5,8), 70.08 (C-6,7), 60.67 (C-9), 111.43 (C-10), 154.36 (C-11), 139.54 (C-12), 107.13 (C-13,17), 148.50 (C-14), 119.24 (C-15), 176.77 (C-16), 145.37 (C-18), 164.21 (C-19), 36.35 (C-20), 8.06 (C-21,22), 49.20–49.67 (C-23,26), 46.03 (C-24,25).

Spectroscopic data of HEC-CIP conjugates **5**, **7** and **8** is shown in supplementary information.

2.4. Methods

2.4.1. Determination of DC of HPC- and HEC-CIP conjugates by UV–Vis spectrophotometry

DC (mg of drug/100 mg of prodrug) of conjugates was calculated using UV–Vis spectrophotometry. In a typical procedure, standard solutions of CIP were prepared in 0.1 N aq. NaOH to construct a calibration curve at 272 nm (λ_{max} of CIP). Then each conjugate (10 mg) was hydrolyzed in 0.1 N aq. NaOH (10 mL) for 8 h at 80 °C with continuous stirring.

The solution was filtered and the volume of the filtrate was made up to 10 mL with 0.1 N aq. NaOH solution. Different dilutions of hydrolyzed sample were made with 0.1 N aq. NaOH solution and their UV absorbance values were recorded. DC of each CIP prodrug was determined using the standard calibration curve.

2.4.2. Determination of DS of conjugates by acid-base titration

Acid-base titrimetry was used to calculate DS(CIP) of HPC and HEC conjugates. In this method, an accurately weighed amount (100 mg) of each prodrug was hydrolyzed in 0.1 N aq. NaOH (100 mL) at 80 °C overnight. The saponified reaction mixture was titrated against HCl (0.01 M) to the colorimetric end point using phenolphthalein indicator. DS was then calculated using Eq. (1);

$$DS = \frac{nNaOH \times Mw_{RU}}{M_S - (Mw_E \times nNaOH)} \quad (1)$$

where, *n.NaOH* is number of moles of NaOH left after saponification, Mw_{RU} is the molar mass of the polymer repeat unit, *Ms.* is the mass of sample, and Mw_E is the molar mass of ester functionality.

2.4.3. Transmission electron microscopy (TEM)

Self-assembly behavior of CIP prodrugs at a DMSO/H_2O interface was investigated by TEM. In a typical experiment, a weighed amount (20 mg) of conjugate was dissolved in DMSO (5 mL) and dialysed against milli-Q water (18.2 MΩ at 25 °C) for 3 days. The suspension obtained was diluted with milli-Q water and drop-casted on carbon coated TEM grids (Cu-200 CK) for characterization using a Philips EM420 electron microscope.

2.4.4. Size exclusion chromatography (SEC)

Molecular weight distributions of HPC- and HEC-CIP conjugates were determined using SEC. A mixture of 0.05 M NaH_2PO_4 and 0.25 M NaCl with pH 7 was used as eluent with flow rate of 0.5 mL min^{-1}. PL Aquagel-OH 40 and PL Aquagel-OH 60 8 μm columns (Agilent) were used with pullulan as an internal standard.

2.4.5. CIP release from HPC- and HEC-CIP conjugates and release kinetics

A dialysis bag method was used to study CIP release from prodrugs. In a typical procedure, an accurately weighed quantity (50 mg) of prodrug was dissolved separately in simulated gastric and intestinal fluids (SGF; pH 1.2 & SIF; pH 7.4, 5 mL) and sealed in separate cellophane dialysis bags (MWCO 14 kDa). Dialysis of each bag was performed against SIF and SGF (900 mL each) separately in a USP II dissolution apparatus maintained at 37 °C and stirring at 100 rpm. At specific time points, sample (2 mL) was withdrawn from the dialysate and sink conditions were maintained by adding an equal volume of fresh release medium. Withdrawn aliquots were suitably diluted and absorbance was recorded at 276 nm for SGF and 270 nm for SIF on a UV–Vis spectrophotometer. Cumulative CIP released from prodrugs was determined from calibration curve of standard. Each hydrolytic drug release experiment was performed thrice to present average values. Pseudo first order kinetic model [32] was applied to hydrolytic drug release data which is shown in Eq. (2).

$$\ln(q_e - q_t) = \ln q_e - kt \quad (2)$$

where q_e and q_t represent equilibrium concentration and concentration at time *t*, respectively while *k* is the rate constant.

A dissolution experiment of pure CIP (control) was also executed under similar conditions.

2.5. Pharmacokinetic studies

2.5.1. Participants and study design

Most common animal models for in vivo studies of newly synthesized oral dosage forms of drugs include rabbits, pigs, dogs and primates. Among these animals, rabbits are more readily available and less costly [33]. Eighteen healthy male albino rabbits (≈2 kg each) were selected for pharmacokinetic studies of HPC-CIP conjugate **2** and HEC-CIP conjugate **6**. Rabbits were divided into three groups; each group with six rabbits. All the rabbits were kept under 12 h light and dark periods and kept under fasting overnight (10 h) with ad libitum access to water. The first group of rabbits was dosed orally with CIP (control; 40 mg), the second and third groups were given 80 and 87 mg of prodrug **2** and **6**, respectively (each containing 40 mg of CIP), using gavage tubes. All animals were kept under observation. They were allowed to take water after 1 h of drug administration and standard green food after 5 h. Ethical protocols of animal studies were approved by the Institutional Animal Ethics Committee, Faculty of Pharmacy, University of Sargodha, Pakistan.

2.5.2. Specimen collection and storage

Blood samples (3–5 mL) from the jugular vein of each rabbit were collected using heparinized disposable syringes at zero time (control group) and at 0.17, 0.5, 1.0, 1.5, 2.0, 4.0, 6.0, 8.0, 12.0, 24.0, 36.0 h (test groups). Each blood sample was centrifuged at 3500 × *g* for 5 min to precipitate blood cells. Supernatant plasma was collected in labeled test tubes which were wrapped in aluminum foil and stored in a freezer at −10 °C before further processing.

2.5.3. Plasma sample preparation

Plasma samples were thawed and to each was added acetonitrile and methanol (1.0 mL each) to precipitate plasma proteins, then the sample was stored for 15 min. Plasma proteins were then separated by centrifugation 3000 × *g* and clear supernatant was extracted by a micropipette and filtered through 0.45 μ nylon syringe filters before processing for HPLC/UV analysis.

2.5.4. Evaluation of bioavailability and pharmacokinetics

Plasma concentration vs. time curves were plotted using Microsoft Excel® 2010. The linear trapezoidal method [34] was used to calculate different pharmacokinetic parameters such as area under the curve from time zero to time t (AUC_{0-t}), area under the curve from time zero to time infinity ($AUC_{0-\infty}$), peak drug concentration (C_{max}), time to peak drug concentration (t_{max}), half-life of the drug ($t_{½}$), volume of distribution (Vd), and clearance (Cl).

2.6. Antibacterial activity

Antibacterial activity of prodrugs **2** and **6** was investigated against six bacterial strains; *Staphylococcus aureus* (American Type Culture Collection [ATCC] 25,923), *Staphylococcus epidermidis* (ATCC 12228), *Streptococcus pneumoniae* (ATCC 49619), *Escherichia coli* (ATCC 25922), *Pseudomonas aeruginosa* (ATCC 27853) and *Bacillus subtilis* (ATCC 6633) using the paper disc diffusion method [35]. Clinical and Laboratory Standards Institute guidelines were followed for the antibacterial assay. MHA (Mueller-Hilton agar) medium was used for the growth of bacteria. Bacterial suspensions (McFarland standard turbidity = 0.5) were diluted (up to 108 cfu ml^{-1}) with sterile physiological solution. MHA discs (10 cm in diameter) were tagged and soaked homogeneously with respective bacterial suspensions (100 μL) and dried for 5 min. Sterilized Whatman filter paper discs (6 mm in diameter) were soaked with solutions of CIP (control) and prodrugs (test) and placed on the surface of a MHA disc, each disc having a different bacterial culture. The inoculated plates were initially incubated at 4 °C for 2 h and then at 37 °C for 24 h. The antibacterial activity of each sample (control & test) was examined by measuring the diameter (mm) of the

Table 1
Reaction conditions and results of synthesis of HPC-CIP (**1–4**) and HEC-CIP (**5–8**) conjugates.

Conjugate	Molar Ratio[a]	Yield (%)	DC[b]	DS(CIP)[c]	DS(CIP)[d]	Solubility
1	1:2:2:4	81	43	0.87	0.85	H_2O, DMF, DMSO, DMAc
2	1:3:3:6	88	50	1.15	1.13	H_2O, DMF, DMSO, DMAc
3	1:4:4:8	85	47	1.02	1.01	H_2O, DMF, DMSO, DMAc
4	1:5:5:10	83	45	0.94	0.92	H_2O, DMF, DMSO, DMAc
5	1:2:2:4	80	37	0.51	0.48	H_2O, DMF, DMSO, DMAc
6	1:3:3:6	86	46	0.75	0.72	H_2O, DMF, DMSO, DMAc
7	1:4:4:8	84	39	0.61	0.58	H_2O, DMF, DMSO, DMAc
8	1:5:5:10	82	41	0.56	0.54	H_2O, DMF, DMSO, DMAc

[a] HPC/HEC:CIP:TsCl:TEA.
[b] DC calcd. by UV–Vis spectroscopy at λmax 272 nm.
[c] DS calcd. from UV–Vis data. DS.
[d] Calcd. by acid base titration.

inhibition zone formed. The assay was performed thrice and results are presented as means with standard errors.

2.7. Cytotoxicity study

Cytotoxicity profiles [36] of the prodrugs **2** and **6** were examined using a 3-(4, 5 dimethylthiazole 2 yl) 2, 5 diphenyltetrazolium bromide (MTT) assay [37]. In a typical experiment, cell lines (L929, fibroblasts) were nurtured in a mixture of α MEM, 1% penicillin and streptomycin solution, fetal bovine serum (10% (*v*/v), and fungizone (2.5 μg mL^{-1}). L929 Cells were seeded (3×10^3 cells per well) in 96-well culture plates and subsequently incubated in a humidified incubator at 37 °C with 5% CO_2 atmosphere. Culture plates were inoculated with aqueous solutions of prodrugs **2** and **6** (50, 100, 150, 200 and 250 μg mL^{-1}) for 24, 48 and 72 h. After the specified time intervals, supernatants from each well were removed and 10 μL of MTT solution (0.5 mg mL^{-1}) was added to each well. The culture plates were again incubated at 37 °C for 4 h. After incubation, MTT solution was removed from each well and DMSO (100 μL) was added to dissolve crystals of formazan. Then absorbance of each sample solution was recorded at 570 nm on a PowerWave™ Microplate spectrophotometer (BioTek, USA). The viability percentage of cells was calculated by using Eq. (3).

$$\%Viability = \frac{A_T}{A_C} \times 100 \tag{3}$$

where, A_T and A_C are the optical densities of treated and control cells, respectively.

2.8. Statistical analysis

Statistical analyses were performed using GraphPad Prism 5.0 (GraphPad Software Inc., La Jolla, CA, USA) and data analyses were executed with one-way ANOVA followed by Dunnett's multiple-comparison test. *P*-values < 0.05 were considered to be statistically significant. All data was expressed as mean ± SD.

3. Results and discussion

3.1. Prodrug synthesis and spectroscopic characterization

MPDs (**1–8**) were prepared by reacting CIP with the hydrophilic cellulose ether derivatives HPC and HEC. TsCl was used as carboxylic acid

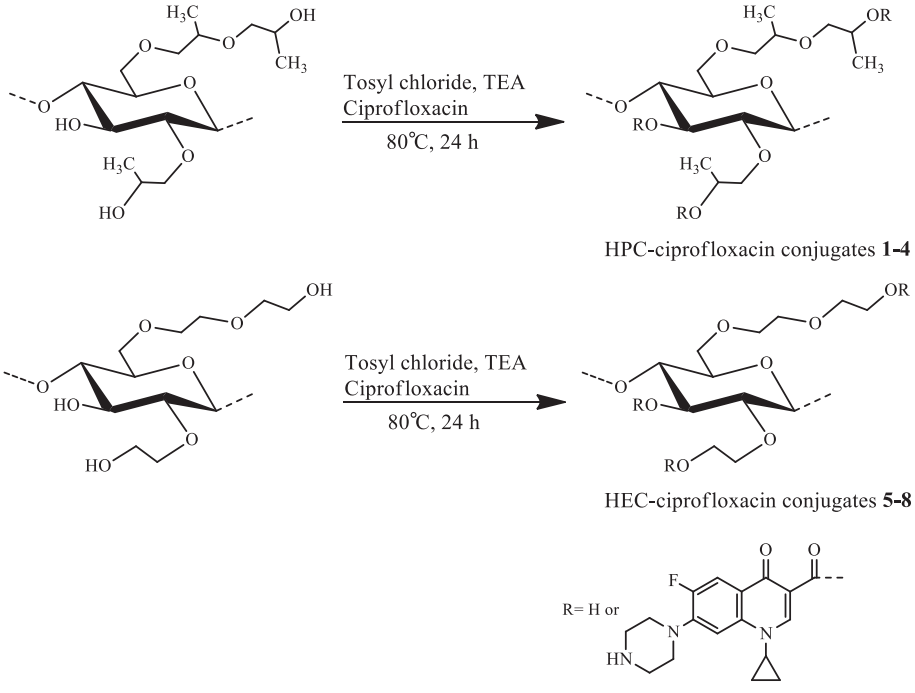

Scheme 1. Synthesis of CIP prodrugs as HPC-CIP **(1–4)** and HEC-CIP **(5–8)** conjugates.

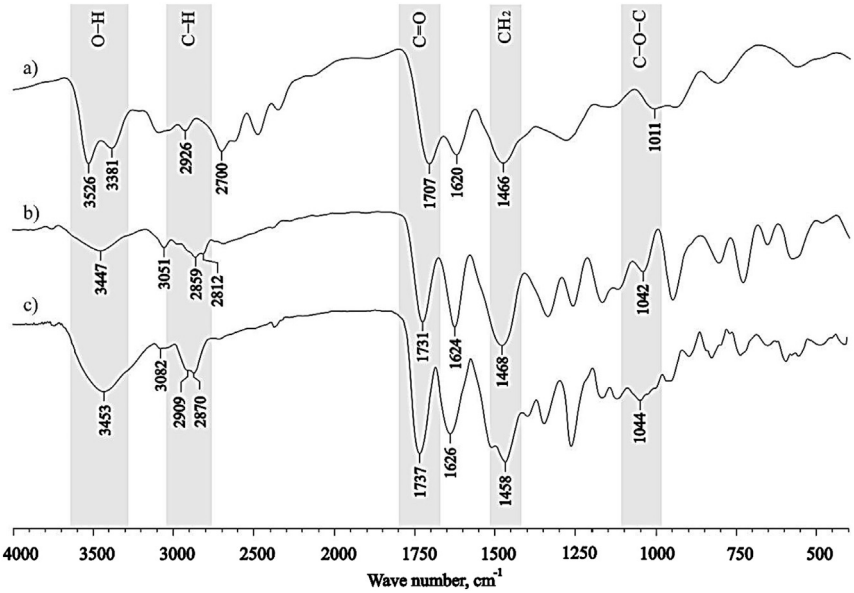

Fig. 1. Overlay FT-IR (KBr) spectra of CIP (a) HPC-CIP conjugate **2** (b) and HEC-CIP conjugate **6** (c).

activating agent for synthesis of the CIP esters, with TEA used as acid scavenger. All CIP MPDs (**1–8**) were soluble in water and various organic solvents.

HPC–CIP conjugates **1–4** contained CIP DC of 43–50 mg/100 mg conjugate by UV–Vis spectrometry, using a standard curve, corresponding to DS(CIP) values of 0.87–1.15. Likewise, HEC–CIP conjugates **5–8** showed had DC 37–46 mg/100 mg conjugate, corresponding to DS (CIP) of 0.51–0.75. DC values were also measured using an HPLC/UV method and were found to be in good agreement with those obtained by UV–Vis method. DS(CIP) of HPC and HEC conjugates (**1–8**) was also evaluated by an acid-base titration method. HPC-CIP conjugates (**1–4**) showed DS(CIP) 0.85–1.13, whereas HEC-CIP conjugates (**5–8**) had DS(CIP) of 0.48–0.72. Table 1 summarizes yield, DC, DS, and solubility of CIP conjugates synthesized using different drug to polymer mole ratios, and reaction strategy is summarized in Scheme 1.

FT-IR spectra of the CIP conjugates showed distinctive ester carbonyl stretch absorbances in the range of 1729–1733 cm^{-1} (HPC-CIP, **1–4**), and 1732–1737 cm^{-1} (HEC-CIP, **5–8**). Carbonyl stretches of the free

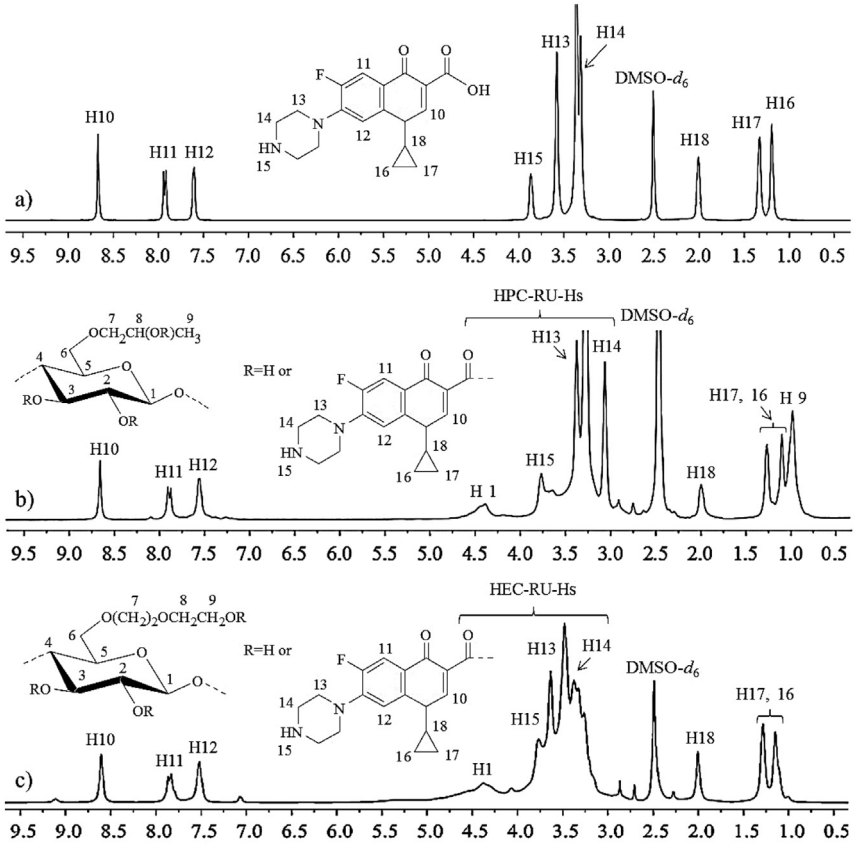

Fig. 2. ^{1}H NMR spectra (500 MHz, DMSO d_6) of CIP (a), HPC-CIP conjugate **2** (b) and HEC-CIP conjugate **6** (c).

CIP carboxylic acid were observed at 1707 cm^{-1} whereas, carbonyl absorbances of the esters were noted at 1731 and 1737 cm^{-1} in HPC-CIP conjugate **2** and HEC-CIP conjugate **6**, respectively. Fig. 1 displays overlay FT-IR spectra of CIP, HPC-CIP conjugate **2** and HEC-CIP conjugate **6**.

In the ^{1}H NMR (500 MHz, DMSO d_6) spectrum of HPC-CIP conjugate **2**, aromatic protons (H-10, H-11 and H-12) of CIP appeared at δ 8.62, 7.87 and 7.54 ppm, respectively. Piperazine ring proton (H-13, H-14 and H-15) signals were found at δ 3.37, 3.06 and 3.76 ppm, respectively, overlapped with HPC backbone protons at δ 2.85–4.74 ppm, whereas cyclopropyl ring proton (H-16 and H-17) signals appeared at δ 1.10 and 1.28 ppm, respectively, overlapping with H-9 of HPC at δ 0.99 ppm. H-18 of the cyclopropyl ring appeared further downfield, at δ 2.06 ppm, analogous to CIP itself and due to greater proximity to electron-poor carbons. The ^{1}H NMR spectrum (DMSO d_6) of HEC-CIP conjugate **6** showed aromatic ring protons (H-10, 11 and 12) of CIP at δ 8.66, 7.86 and 7.51 ppm, respectively. Piperazine ring proton (H-13, 14 and 15) signals appeared at δ 3.65, 3.36 and 3.78 ppm overlapping with the HEC backbone proton region at δ 3.05–4.75 ppm. Cyclopropyl ring protons (H-16 and H-17) signals were detected at δ 1.19 and 1.32 ppm, respectively while H-18 of the cyclopropyl ring was again further downfield at δ 2.01 ppm. ^{1}H NMR spectra of CIP, HPC-CIP conjugate **2,** and HEC-CIP conjugate **6** are given in Fig. 2a, b and c, respectively for comparison. The absence of carboxylic group proton signals in the spectra of conjugates **2** and **6** also confirmed successful esterification of CIP with HPC and HEC.

In the ^{13}C NMR spectrum of HPC-CIP conjugate **2**, shifting of the acid carbonyl (C-19) resonance from δ 166.63 to 163.74 ppm confirms formation of the prodrug ester linkage. The ketone carbonyl (C-16) was observed at δ 176.80 ppm. Carbon signals of the aromatic region of CIP in HPC-CIP conjugate **2** were detected at δ 111.56–148.56 (C-10-18) ppm (Fig. 3b). Carbon signals of the HPC repeating unit appeared at δ 102.69 (C-1), 65.45 (C-6 and C-8), 74.91 (C-2 and C-7), 76.53–82.78 (C-3-5) ppm. Moreover, carbon signals of the methyl groups of the HPC repeating unit were measurable at δ 21.49–20.67 ppm. Likewise, in the ^{13}C NMR spectrum of HEC-CIP conjugate **6**, the upfield shift of the acid carbonyl (C-19) signal from δ 166.63 to 164.21 ppm as an ester carbonyl showed successful esterification of CIP with HEC. Carbon signals of conjugated CIP and HEC were also detectable and are shown in a self-explanatory way in the spectra. ^{13}C NMR spectra of CIP, HPC-CIP conjugate **2** and HEC-CIP conjugate **6** are given in Fig. 3a–c for comparison.

3.2. Transmission electron microscopy

Conjugation of hydrophobic drug molecules with hydrophilic biopolymers such as HPC and HEC leads to the formation of amphiphilic prodrugs which exhibit self-assembly behaviour at a DMSO/H_2O interface. The hydrophobic/hydrophilic balance of HPC-CIP and HEC-CIP conjugates was tuned by varying the mole ratios of appended drug, to observe the impact upon their self-assembly behaviour. Among HPC-CIP conjugates, only conjugate **2** showed defined nanoparticulate self-assembly behavior. Fig. 4a and b show TEM images of nanoparticles in the range 150–300 nm for conjugate **2** at the solvent interface. Among HEC-CIP conjugates, only conjugate **6** showed distinct nano-assembly behavior (Fig. 4c and d). TEM images confirm the fabrication of nanoparticles for conjugate **6** in the size range 180–250 nm. Self-assembling of these conjugates to nanoparticles may be attributed to their balanced amphiphilic nature.

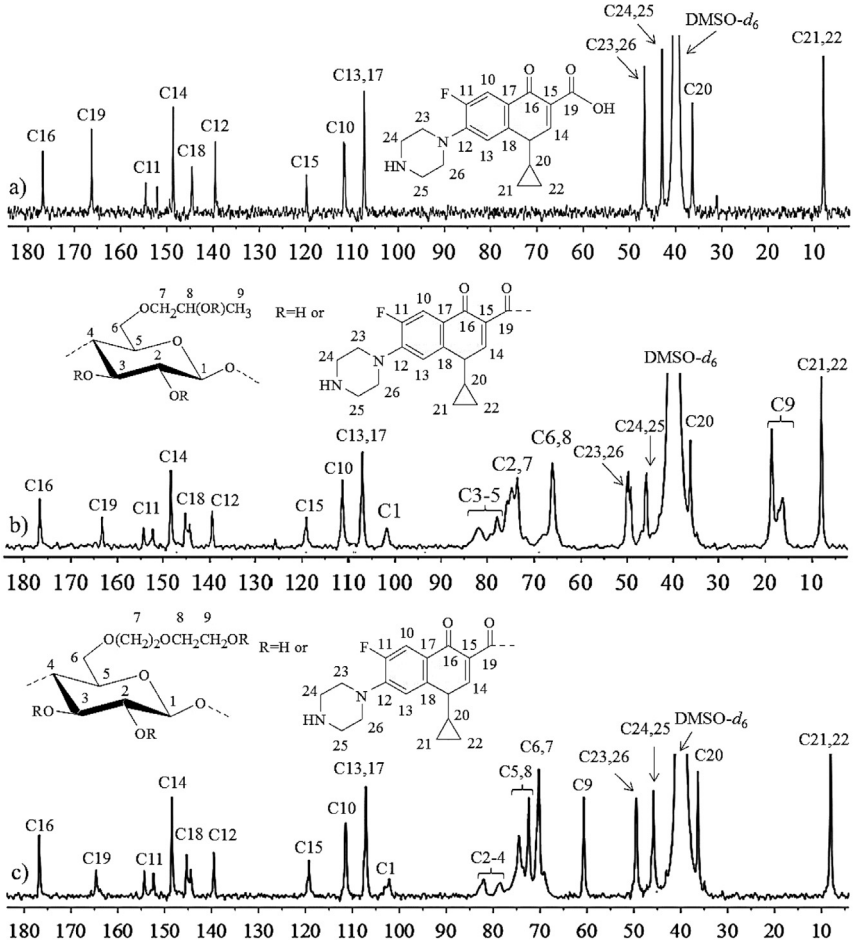

Fig. 3. ^{13}C NMR spectra (400 MHz, DMSO d_6, ca. 5000 scans) of CIP (a), HPC-CIP conjugate **2** (b) and HEC-CIP conjugate **6** (b).

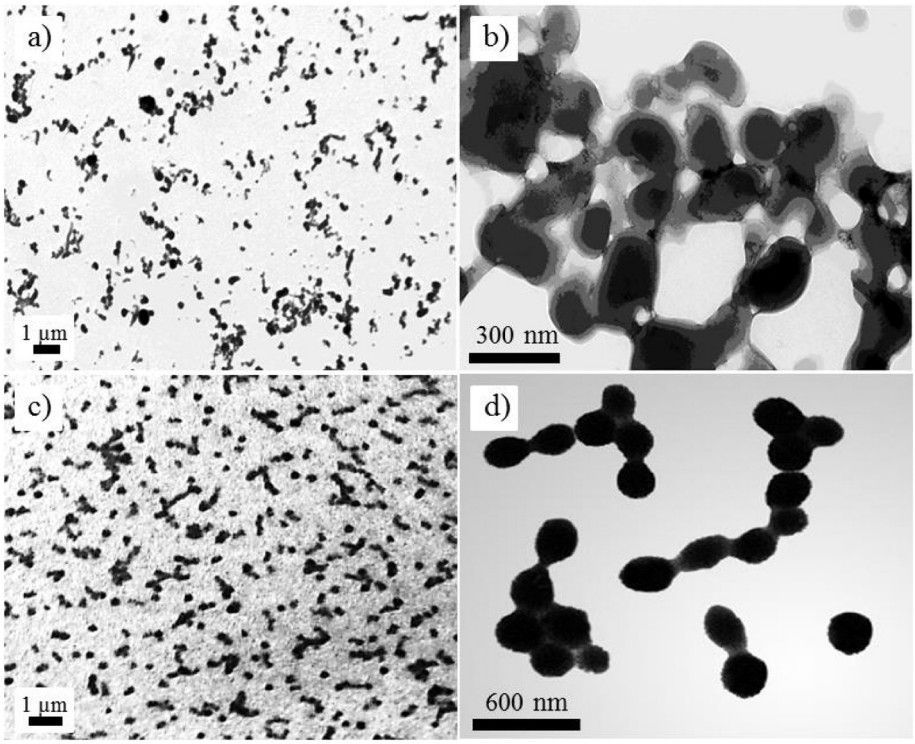

Fig. 4. TEM images of HPC-CIP conjugate **2** (a, b) and HEC-CIP conjugate **6** (c, d).

3.3. Size exclusion chromatography

SEC was performed to study molecular mass distributions of HPC, HEC, HPC-CIP conjugate **2,** and HEC-CIP conjugate **6**. The M_w values calculated for conjugate **2** and **6** were 1.097×10^5 and 3.1×10^5 g mol^{-1}, respectively, whereas unmodified HPC and HEC showed M_W values of 1.16×10^5 and 3.6×10^5 g mol^{-1}, respectively. Degree of polymerization (DP) values were found to be 152 and 607 for conjugates **2** and **6**, respectively. SE chromatograms of HPC, HEC, conjugates **2** and **6** are shown in Fig. 5.

3.4. In vitro drug release and kinetics

In vitro release of CIP from HPC-CIP conjugate **2** and HEC-CIP conjugate **6** was performed in SGF (pH 1.2) and SIF (pH 7.4) at 37 °C using a dialysis bag method. HPC-CIP conjugate **2** releaased substantially more CIP (43%) in SIF than in SGF (15%) in the first 6 h. HEC-CIP conjugate **6** showed similar behavior over that time frame, releasing only 16% CIP in SGF as compared to 46% in SIF. The hydrolytic release profiles of CIP from conjugates **2** and **6** in SGF and SIF are shown in Fig. 6a and b, respectively. These CIP release profiles were consistent with reported release profiles of other polysaccharide based conjugates [38–40]. Higher drug release rate at pH 7.4 from conjugates **2** and **6** suggests potential for intestine targeted prodrug design for CIP. The dissolution profile of pure CIP powder was also investigated under the same conditions, and it was noted that >90% drug dissolved within 10 min, in contrast to the slower CIP release profiles of the esterified MPDs, indicating that the dialysis membrane did not delay the release of pure drug.

A pseudo first order kinetic model was applied to the hydrolytic release data of conjugate **2** and **6**. The linearity of the graphs plotted of ln $(q_e - q_t)$ vs. time established the good fit of the model to the release data. Moreover, release of CIP from conjugate **2** and **6** increased with passage of time. Fig. 6c and d displays the pseudo first order release kinetic plots of conjugates **2** and **6**, respectively. Fig. 6e and f elucidate the simulated release profile of CIP from conjugates **2** and **6**, respectively at pH 1.2, 6.8 and 7.4. Conjugate **2** showed about 4, 39 and 73% CIP release at pH 1.2, 6.8 and 7.4, respectively. Similarly, conjugate **6** exhibited almost 4, 41 and 74% release at pH 1.2, 6.8 and 7.4, respectively.

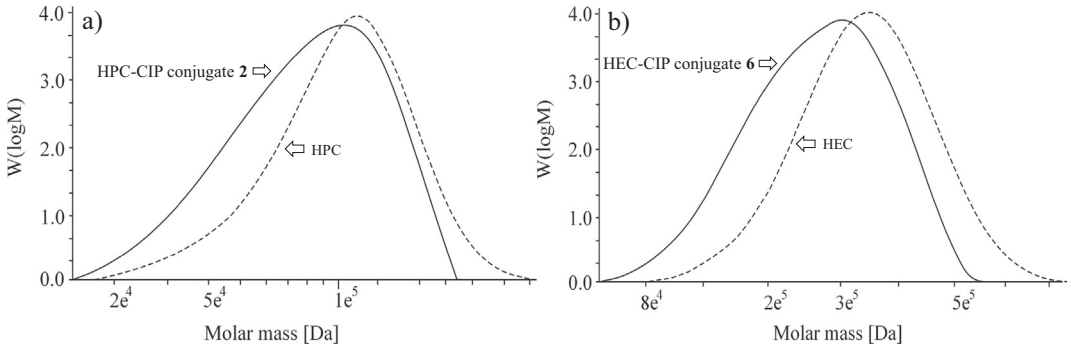

Fig. 5. SE chromatograms of HPC, HPC-CIP conjugate **2** (a) and HEC, HEC-CIP conjugate **6** (b).

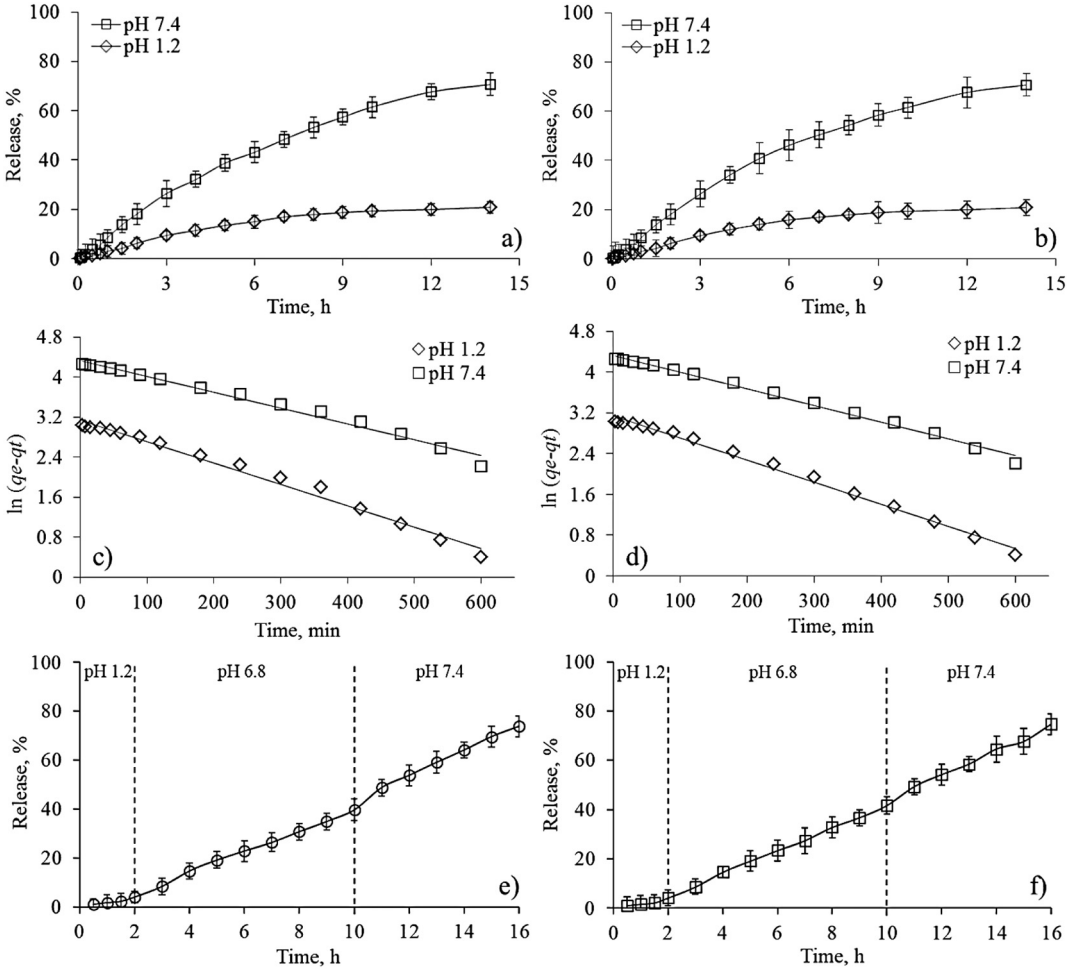

Fig. 6. Overlay plots of (a, b) CIP release in SGF and SIF, (c, d) Pseudo first order kinetics of hydrolytic release of CIP in SGF and SIF and (e, f) simulated release of CIP at pH 1.2, 6.8 and 7.4 from HPC-CIP conjugate **2** and HEC-CIP conjugate **6**, respectively.

3.5. Pharmacokinetic studies

A reverse phase HPLC method was developed and validated as per ICH guidelines for bioavailability and pharmacokinetic studies of CIP release from the CIP conjugates in a rabbit model, using CIP as control. The method validation parameters evaluated are listed in Table S1.

The overlay plots of plasma concentration vs. time for CIP, HPC-CIP conjugate **2,** and HEC-CIP conjugate **6** are shown in Fig. 7.

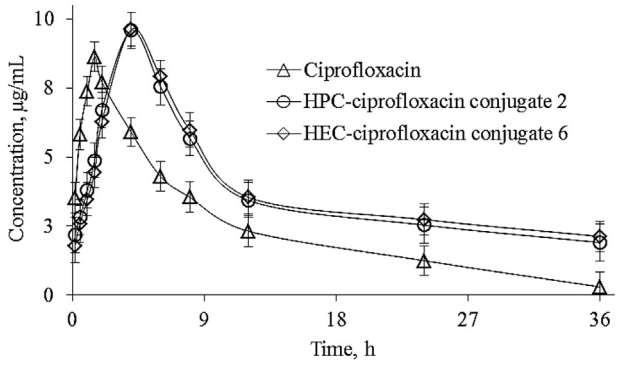

Fig. 7. Mean plasma concentrations vs. time curves after oral administration of CIP, HPC-CIP conjugate **2,** and HEC-CIP conjugate **6** to rabbits.

HPC-CIP conjugate **2** had t_{max} 4.0 and $t_{1/2}$ 10.87 h; much higher as compared to those for CIP (1.5 h (t_{max}) and 4.16 h ($t_{1/2}$)). The significant increase in half-life value of CIP from conjugate **2** supports the value of the conjugate for sustained CIP release. The $AUC_{0-\infty}$ value of conjugate **2** was 164.53 ± 5.13 h µg mL^{-1}, almost double that of the pure drug (90.16 ± 3.21 h µg mL^{-1}). Thus, CIP bioavailability was also strongly enhanced from HPC-CIP conjugate **2**. HEC-CIP conjugate **6** had t_{max} 4.0 h, and $t_{1/2}$ 11.71 h, surprisingly similar to the values for the HEC conjugate. Conjugate **6** afforded an $AUC_{0-\infty}$ value of 175.78 ± 6.19 h µg mL^{-1}, or a nearly two-fold enhancement of bioavailability vs. pure CIP. Full pharmacokinetic data for each conjugate can be found in Table 2. The longer $t_{1/2}$ of CIP from conjugate **2** and **6** also indicates that it provides levels above the MIC (minimum inhibitory concentration) for longer time interval hence providing the benefit of lower dosage frequency. Neither HPC nor HEC, being high molecular weight cellulose ether derivatives

Table 2
Pharmacokinetic data after single oral doses of HPC-CIP conjugate **2** (80 mg) and HEC-CIP conjugate **6** (87 mg) containing amounts of CIP equal to that in pure drug (40 mg).

Parameter	CIP	CIP from HPC-CIP conjugate **2**	CIP from HEC-CIP conjugate **6**
t_{max} (h)	1.5	4.0	4.0
C_{max} (µg mL^{-1})	8.63 ± 0.26	9.59 ± 0.36	9.63 ± 0.72
$t_{1/2}$ (h)	4.16 ± 0.53	10.87 ± 0.87	11.71 ± 0.81
$AUC_{0-\infty}$ (h µg mL^{-1})	90.16 ± 3.21	164.53 ± 5.13	175.78 ± 6.19
Vd (L kg^{-1})	3.95 ± 0.8	2.86 ± 0.07	2.88 ± 0.04
Cl (L h^{-1})	0.33 ± 0.13	0.18 ± 0.01	0.17 ± 0.01

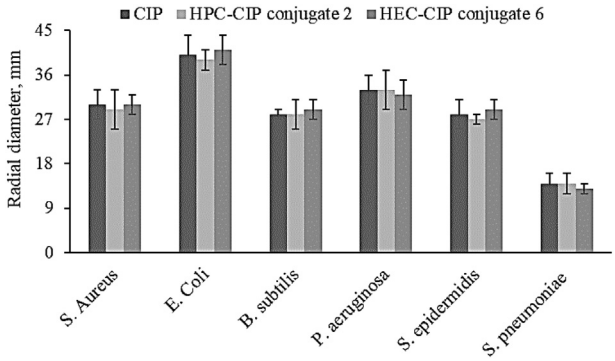

Fig. 8. Inhibitory zones (radial diameters) of CIP, HPC-CIP conjugate **2** and HEC-CIP conjugate **6** against different bacterial strains.

with many hydrogen bond donors and acceptors, do not have the ability to permeate through the epithelium, hence the drug must enter circulation after the prodrug hydrolyzes in the small intestine. Moreover, we postulate that dissolution and hydrolysis rates of prodrug determine its pharmacokinetic profile. The nearly equal C_{max} values observed for the two prodrugs vs. that of pure CIP are interesting given the slower release from the prodrugs, and could be due to higher dissolution rates of the prodrugs than for the more hydrophobic pure CIP.

3.6. Bioassays

3.6.1. In vitro antibacterial activity

The antibacterial activities of HPC-CIP conjugate **2** and HEC-CIP conjugate **6** were tested using a disc diffusion method. Each prodrug had antimicrobial activity equivalent to that of unmodified CIP against bacteria including *S. aureus*, *E. coli*, *B. subtilis*, *P. aeruginosa*, *S. epidermidis*, and *S. pneumoniae*. Fig. 8 shows the inhibiting zone diameters of unmodified CIP and prodrugs **2** and **6** against these bacterial strains. The results indicate that the biological activity of CIP is not compromised by conjugation to HPC and HEC. All experiments were performed in triplicate and mean values with standard error are given in Table 3.

3.6.2. In vitro cytotoxicity assay

In vitro cytotoxicity of HPC-CIP conjugate **2** and HEC-CIP conjugate **6** was assessed by MTT assay, a colorimetric method used to measure the metabolic activity of cells. L929 (fibroblasts) cell lines were exposed to different concentrations of conjugate **2** and **6** for 24, 48 and 72 h. Fig. 9a–c shows cytotoxicity results in terms of percent inhibition of mitochondrial oxidoreductase enzyme. It was observed that both conjugates showed no cytotoxicity at 150 μg mL^{-1} concentration even after 72 h. Nevertheless, higher concentrations of both conjugates exhibited substantial reductions in cell viability. Since the tested concentrations (50–250 μg mL^{-1}) are higher than those achieved after recommended oral dosage form of CIP, these prodrugs can be considered safe for use at normal CIP doses.

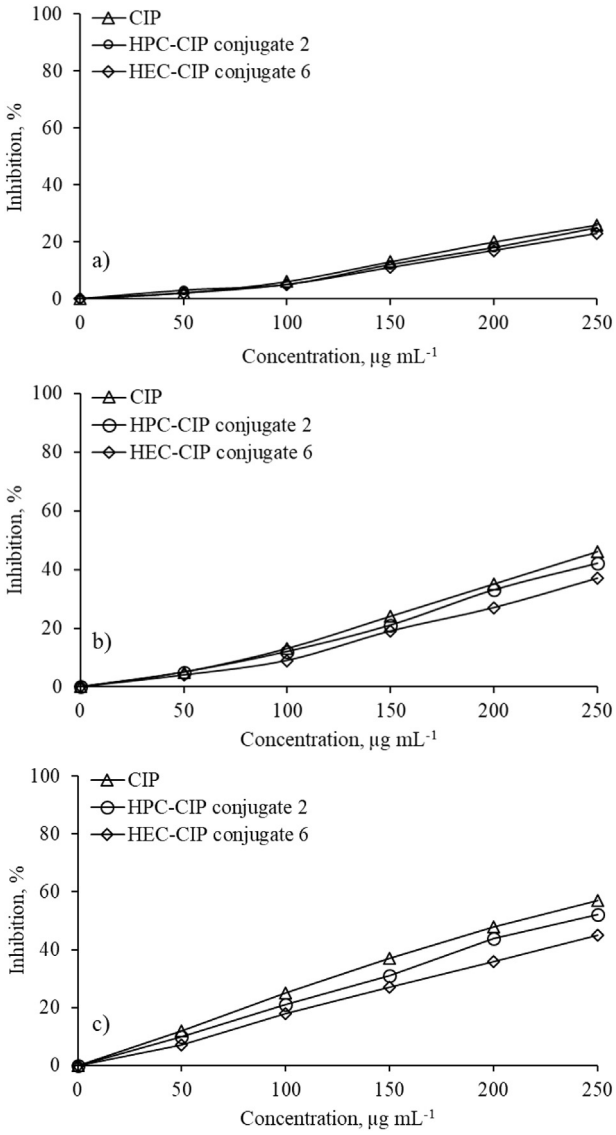

Fig. 9. Cytotoxic effect (% inhibition) of different concentrations of CIP, HPC-CIP conjugate **2** and HEC-CIP conjugate **6** on cell line L929 after (a) 24, (b) 48 and (c) 72 h incubation periods.

4. Conclusion

One pot reaction methodology was adopted for the syntheses of HPC- and HEC-based MPDs of CIP, resulting in water- and organic-soluble prodrugs. Pharmacokinetic profiles of orally administered prodrugs to rabbits revealed higher CIP bioavailability due to their delayed and extended release behavior. Their in vitro and in vivo CIP release profiles suggest that these prodrugs are promising candidates for ileum and colon targeted drug delivery. The prodrugs were relatively stable at acidic stomach pH, due to slower acid catalyzed ester hydrolysis. This could also be a valuable property in some cases by reducing interaction with co-administered proton pump inhibitors or other antacids. Preliminary cytotoxicity studies indicated the non-toxic nature of these conjugates at normal CIP dosing levels. Antibacterial assays confirmed that conjugation of CIP with HPC and HEC did not hamper its antibacterial activity. The higher bioavailability of CIP from prodrugs makes them plausible for once-daily formulations.

Table 3
Antibacterial activity in terms of inhibition zone diameter (mm) of CIP, HPC-CIP conjugate **2,** and HEC-CIP conjugate **6** using disc diffusion method.

Sample	*S. aureus*	*E. coli*	*B. subtilis*	*P. aeruginosa*	*S. epidermidis*	*S. pneumoniae*
CIP	30 ± 3	40 ± 4	28 ± 1	33 ± 3	28 ± 3	14 ± 2
Conjugate **2**	29 ± 4	39 ± 2	28 ± 3	33 ± 4	27 ± 1	14 ± 2
Conjugate **6**	30 ± 2	41 ± 3	29 ± 2	32 ± 3	29 ± 2	13 ± 1

Acknowledgments

M. Amin and N.S. Abbas acknowledge the Higher Education Commission of Pakistan for financial support under the IRSIP program. N. S. Abbas also appreciates financial support from the Higher Education Commission of Pakistan under the "Indigenous 5000 PhD fellowships program". We acknowledge Ashland Inc., Covington, KY, USA for their generous gift of HEC. We also acknowledge STANDPHARM Pakistan (Pvt) Ltd. Lahore for a generous gift of CIP.

Appendix A. Supplementary data

Supplementary data to this article can be found online at https://doi.org/10.1016/j.ijbiomac.2018.02.142.

References

[1] V.T. Andriole, Use of quinolones in treatment of prostatitis and lower urinary tract infections, Eur. J. Clin. Microbiol. Infect. Dis. 10 (4) (1991) 342–350.
[2] A.P. MacGowan, M. Wootton, H.A. Holt, The antibacterial efficacy of levofloxacin and ciprofloxacin against Pseudomonas aeruginosa assessed by combining antibiotic exposure and bacterial susceptibility, J. Antimicrob. Chemother. 43 (1999) 345–349.
[3] R. Mather, L.M. Karenchak, E.G. Romanowski, R.P. Kowalski, Fourth-generation fluoroquinolones. New weapons in the arsenal of ophthalmic anti-infectives, Am J. Ophthalmol. 133 (2002) 463–466.
[4] M.I. Andersson, A.P. MacGowan, Development of the quinolones, J. Antimicrob. Chemother. 51 (2003) 1–11.
[5] S. Heeb, M.P. Fletcher, S.R. Chhabra, P. Diggle, P. Williams, M. Cámara, Quinolones: from antibiotics to autoinducers, FEMS Microbiol. Rev. 35 (2011) 247–274.
[6] X. Yu, G.L. Zipp, G.W.R. Davison, The effect of temperature and pH on the solubility of quinolone compounds: estimation of heat of fusion, Pharm. Res. 11 (1994) 522–527.
[7] J.L. Va'zquez, M. Berlanga, S. Merino, O. Dome'nech, M. Viñas, M.T. Montero, J. Herna'ndez-Borrell, Determination by fluorimetric titration of the ionization constants of ciprofloxacin in solution and in the presence of liposomes, Photochem. Photobiol. 73 (2001) 14–19.
[8] A. Tsuji, H. Sato, Y. Kume, I. Tamai, E.E. Okezaki, O. Nagata, H. Kato, Inhibitory effects of quinolone antibacterial agents on g-aminobutyric acid binding to receptor sites in rat brain membranes, Antimicrob. Agents Chemother. 32 (1988) 190–194.
[9] S. Harder, U. Fuhr, D. Beermann, H. Staib, Ciprofloxacin absorption in different regions of the human gastrointestinal tract. Investigations with the HF-capsule, Br. J. Clin. Pharmacol. 30 (1990) 35–39.
[10] K.I. Plaisance, G.L. Drusano, A. Forrest, C. Bustamante, H.C. Standiford, Effect of dose size on bioavailability of ciprofloxacin, Antimicrob. Agents Chemother. 31 (1987) 956–958.
[11] T.A. Tartaglione, A.C. Raffalovich, W.J. Poynor, A. Espinel-Ingroff, T.M. Kerkering, Pharmacokinetics and tolerance of ciprofloxacin after sequential increasing oral doses, Antimicrob. Agents Chemother. 29 (1986) 62–66.
[12] G. Hoffken, H. Lode, C. Prinzing, K. Borner, P. Koeppe, Pharmacokinetics of ciprofloxacin after oral and parenteral administration, Antimicrob. Agents Chemother. 27 (1985) 375–379.
[13] P.C. Sharma, M. Piplani, M. Mittal, R. Pahwa, Insight into prodrugs of quinolones and fluoroquinolones, Infect. Disord. Drug Targets 16 (2016) 140–161.
[14] C. Florindo, A. Costa, C. Matos, S.L. Nunes, A.N. Matias, C.M. Duarte, L.P.N. Rebelo, L.C. Branco, I.M. Marrucho, Novel organic salts based on fluoroquinolone drugs: synthesis, bioavailability and toxicological profiles, Int. J. Pharm. 469 (2014) 179–189.
[15] N. Von Rosenstiel, D. Adam, Quinolone antibacterials, Drugs 47 (1994) 872–901.
[16] K. Sankula, S. Kota, S. Nissankarrao, Enhancement of dissolution rate of ciprofloxacin by using various solid dispersion techniques, Int. J. Pharm. Res. Health Sci. 2 (2014) 80–86.
[17] F. Dubar, G. Anquetin, B. Pradines, D. Dive, J. Khalife, C. Biot, Enhancement of the antimalarial activity of ciprofloxacin using a double prodrug/bioorganometallic approach, J. Med. Chem. 52 (2009) 7954–7957.
[18] M. Amin, N.S. Abbas, M.A. Hussain, K.J. Edgar, M.N. Tahir, W. Tremel, M. Sher, Cellulose ether derivatives: a new platform for prodrug formation of fluoroquinolone antibiotics, Cellulose 22 (2015) 2011–2022.
[19] M.C. Chung, P.L. Bosquesi, J.L. dos Santos, A Prodrug approach to improve the physico-chemical properties and decrease the genotoxicity of nitro compounds, Curr. Pharm. Des. 17 (2011) 3515–3526.
[20] V.J. Stella, Prodrugs: some thoughts and current issues, J. Pharm. Sci. 99 (2010) 4755–4765.
[21] S. Dhaneshwar, G. Vadnerkar, Rational design and development of colon-specific prodrugs, Curr. Top. Med. Chem. 11 (2011) 2318–2345.
[22] M.A. Hussain, K. Abbas, M. Sher, M.N. Tahir, W. Tremel, M.S. Iqbal, M. Amin, M. Badshah, Macromolecular prodrugs of aspirin with HPMC: a nano particulate drug design, characterization, pharmacokinetic studies, Macromol. Res. 19 (2011) 1296–1302.
[23] M.A. Hussain, K. Abbas, M. Amin, B.A. Lodhi, S. Iqbal, M.N. Tahir, W. Tremel, Novel high-loaded, nanoparticulate and thermally stable macromolecular prodrug design of NSAIDs based on hydroxypropylcellulose, Cellulose 22 (2015) 461–471.
[24] W. Xu, J. Ding, C. Xiao, L. Li, X. Zhuang, X. Chen, Versatile preparation of intracellular-acidity-sensitive oxime-linked polysaccharide-doxorubicin conjugate for malignancy therapeutic, Biomaterials 54 (2015) 27–86.
[25] D. Li, J. Han, J. Ding, L. Chen, X. Chen, Acid-sensitive dextran prodrug: a higher molecular weight makes a better efficacy, Carbohydr. Polym. 161 (2017) 33–41.
[26] D. Li, J. Ding, X. Zhuang, L. Chen, X. Chen, Drug binding rate regulates the properties of polysaccharide prodrugs, J. Mater. Chem. B 4 (2016) 5167–5177.
[27] N.S. Abbas, M. Amin, M.A. Hussain, K.J. Edgar, M.N. Tahir, W. Tremel, Extended release and enhanced bioavailability of moxifloxacin conjugated with hydrophilic cellulose ethers, Carbohydr. Polym. 136 (2016) 1297–1306.
[28] H. Bundgaard, U. Klixbüll, E. Falch, Prodrugs as drug delivery systems: o-acyloxymethyl, o acyl and n acyl salicylamide derivatives as possible prodrugs for salicylamide, Int. J. Pharm. 30 (1986) 111–121.
[29] K.M. Huttunen, H. Raunio, J. Rautio, Prodrugs-from serendipity to rational design, Pharmacol. Rev. 63 (2011) 750–771.
[30] A. Testa, Prodrugs: bridging pharmacodynamic/pharmacokinetic gaps, Curr. Opin. Chem. Biol. 13 (2009) 338–344.
[31] K. Abbas, M. Amin, M.A. Hussain, M. Sher, S.N.A. Bukhari, K.J. Edgar, Design, characterization and pharmaceutical/pharmacological applications of ibuprofen conjugates based on hydroxyethylcellulose, RSC Adv. 7 (2017) 50672–50679.
[32] S. Lagergren, Zur theorie der sogenannten adsorption gelöster stoffe, Kungliga Svenska Vetenskapsakademiens, Handlingar, vol. 24, 1898 1–39.
[33] Y. Qiu, Y. Chen, G.G. Zhang, L. Yu, R.V. Mantri, Developing Solid Oral Dosage Forms: Pharmaceutical Theory and Practice, second ed. Academic press, 2016.
[34] L. Shargel, S. Wu-Pong, A.B.C. Yu, Introduction to biopharmaceutics and pharmacokinetics, Applied Biopharmaceutics and Pharmacokinetics, 6th EdThe McGraw-Hill Companies Inc., USA, 2012.
[35] A. Bondi, E.H. Spauling, E.D. Smith, C.C. Dietz, A routine method for the rapid determination of susceptibility to Penicilln and other antibiotics, Am J Med Sci 214 (1947) 221–225.
[36] R. Rosario-Meléndez, W. Yu, K.E. Uhrich, Biodegradable polyesters containing ibuprofen and naproxen as pendant groups, Biomacromolecules 14 (2013) 3542–3548.
[37] M.V. Berridge, A.S. Tan, Characterization of the cellular reduction of 3 (4, 5 dimethylthiazol 2 yl) 2, 5 diphenyltetrazolium bromide (MTT): subcellular localization, substrate dependence, and involvement of mitochondrial electron transport in MTT reduction, Arch. Biochem. Biophys. 303 (1993) 474–482.
[38] M. Babazadeh, Synthesis and in vitro evaluation of acrylate-basedmacromolecular prodrugs containing mesalazine for colon-specific drug delivery, Pharma Chem. 6 (2014) 411–419.
[39] M. Babazadeh, M. Sheidaei, S. Abbaspour, L. Edjlali, Synthesis, characterization, and in vitro evaluation of new ibuprofen polymeric prodrugs based on 2 hydroxypropyl methacrylate, Sci. Pharm. 81 (2013) 281–296.
[40] X. Zheng, R.D. Gandour, K.J. Edgar, Probing the mechanism of TBAF-catalyzed deacylation of cellulose esters, Biomacromolecules 14 (2013) 1388–1394.